Morphology-controlled ZnO particles from an ionic liquid precursor

Zhonghao Li,*[a] Qian Yu,[a] Yuxia Luan,[b] Guangshan Zhuang,[a] Runhua Fan,[a] Rui Li[a] and Chengguo Wang[a]

Received 28th May 2009, Accepted 24th July 2009
First published as an Advance Article on the web 14th August 2009
DOI: 10.1039/b910551b

The ionic liquid precursor tetraethylammonium hydroxide (TEAH) acting as the reactant precursor and the solvent is demonstrated to be effective for synthesis of ZnO particles with controlled morphologies: hollow ZnO rods, flower-like ZnO particles constructed by rods with nanoparticle subunits and porous ZnO microspheres assembled from ZnO nanoplates. The formation mechanism of the synthesized particles is discussed according to the experimental results. Room temperature photoluminescence (PL) spectroscopy is measured to reveal the optical property of the as-obtained products.

Introduction

Room-temperature ionic liquids (ILs) are attractive environmentally benign solvents for organic chemical reactions, separations, and electrochemical applications.[1–3] The advantages of ILs in inorganic nanomaterial synthetic processes have been gradually realized and have received increasing attention due to their unique physical and chemical properties, such as large electrochemical window, polar but low interface tension, low interface energies, high thermal stability, and extended hydrogen bond systems.[4–14] Particularly, ionic liquids can act as solvents, reactants, and templates for the fabrication of inorganic materials.[6,7] In some cases, ILs and the structurally related ionic liquid crystals combine these functions and serve as "all-in-one" solvent-reactant-templates, or ionic liquid (crystal) precursors (ILPs and ILCPs, respectively). For example, Taubert *et al.* have used ILCPs for the fabrication of CaF_2 tubes, CuCl plates and Au plates from IL(C)Ps.[15–19] The ILCPs act as the precursor for the inorganic material, as the solvent for the reaction, and also as the template over the final inorganic particle morphology. According to the original ILCPs approach,[15] the concept of fabrication of inorganics from ILPs has been developed.[20,21]

ZnO is an important semiconductor with a direct wide band gap of 3.37 eV and large exciton binding energy of 60 meV at room temperature. It has attracted considerable interest in the past years mainly because of the unique optical and electrical properties, as well as its potential application in optical waveguides, blue light-emitting diodes, solar cells, chemical sensors and photocatalysts, *etc.*[22] The interesting shape-dependent optoelectronic and gas sensing properties of ZnO make researchers explore the facile method of preparing ZnO particles with controlled structures. Until now, various ZnO nanostructures have been prepared by using chemical vapour deposition, thermal evaporating and pyrolysis, hydrothermal and capping agent-assisted wet chemical approaches, *etc.*[23] We have recently shown that the highly hydrated IL tetrabutylammonium hydroxide (TBAH) is an efficient ILP for the fabrication of nanostructured inorganic particles including ZnO.[24–28] Inspired by this, we are interested in understanding the particle formation in other kinds of ionic liquid precursor which have a similar structure to that of the TBAH. Herein we use the ionic liquid tetraethylammonium hydroxide (TEAH), which has as similar structure to TBAH, as an example to demonstrate that ZnO particles with controlled morphologies can be obtained from this ionic liquid precursor. The synthesized nanostructured ZnO particle includes: hollow ZnO rods, flower-like ZnO particles constructed by rods with nanoparticle subunits and porous ZnO microspheres assembled from ZnO nanoplates. These interesting ZnO particles can be obtained just by adjusting the concentration of the reactants, therefore the method provides a facile controlled route for the synthesis. The formation mechanism of the synthesized particles is discussed and room temperature photoluminescence (PL) spectroscopy is measured to reveal the optical property of the as-obtained products.

Experimental

Synthesis

In a typical synthesis, 10 mg of zinc acetate dihydrate (Tianjin Guangcheng reagent company) was dissolved in 0.5 g of tetraethyl ammonium hydroxide aqueous solution (TEAH, 25% w/w, Shanghai Yongsheng reagent company) in a 10 ml tube. Then, the tube with the solution was heated to 80 °C for 2 h in air. The products were recovered by repeated centrifugation, washed with water and ethanol, respectively, and dried at 60 °C for 5 h. The procedure for the products recovered at other conditions is similar to the above although the amount of zinc acetate dihydrated is different or a certain amount of water is added to the TEAH solution.

Characterization

X-Ray diffraction was done on a Rigaku Dmax-rc X-ray diffractometer with Ni filtered Cu Kα radiation. SEM was performed on a Hitachi SU-70 FESEM operated at 10 kV. TEM was carried out on a Hitachi H-800 transmission electron

[a]*Key laboratory for Liquid-Solid Structural Evolution and Processing of Materials (Ministry of Education), Schoolof Materials Science and Engineering, Shandong University, Jinan, Shandong Province, 250061, P. R. China. E-mail: zhonghaoli@sdu.edu.cn; Fax: +(86) 531-88392315; Tel: +(86) 531-88392112*
[b]*School of Pharmaceutical Sciences, Shandong University,*

microscope at an accelerating voltage of 150 kV. Room temperature photoluminescence spectra were recorded with a Cary Eclipse fluorescence spectrophotometer (Varian, Australia) equipped with a xenon lamp and quartz carrier at room temperature.

Results and discussion

Fig. 1 shows the XRD pattern of ZnO particles prepared by a reaction of 10 mg zinc acetate dihydrate in 0.5 g TEAH ionic liquid with 0.5 g added water under 80 °C for 2 h. All diffraction peaks in the range $20 < 2\theta < 80°$ can be indexed as the hexagonal ZnO, which is in good accordance with the values on the standard card (JCPDS 36-1451). The XRD results confirm the formation of pure ZnO powders and the product is well crystallized. The intensity of 100 reflexion is low, which indicates that the (100) planes are not parallel to the substrate.

Fig. 2a shows typical SEM images of the ZnO products precipitated at 10 mg zinc acetate dihydrate in 0.5 g TEAH solution with 0.5 g added water, manifesting the formation of ZnO rods. The average length of these particles is *ca.* 1 μm and the diameter of the rods ranges from *ca.* 300 to 400 nm. The enlarged SEM images shown in Fig. 2b suggest that the rods usually contain a central channel resulting in a hollow rod structure. Fig. 2c shows a typical TEM image of a single rod which clearly displays the tip structure of the rod. The selected area electron diffraction pattern of the rod crystal shown in the insert of Fig. 2c suggests that the rod has a single crystalline structure along the [0001] direction.

In order to understand the formation process of the ZnO hollow rods and their growth mechanism, time-dependent shape evolution studies are conducted for the products recovered at different reaction time. It is found the solution becomes slightly turbid when the reaction time is 5 min. The TEM image of the product recovered at this stage is displayed in Fig. 3a. It shows that there are rod particles forming at the initial stage. For the reaction proceeding for 10 min, the products are still in rod shape while there are some dark dots (nanoparticles) in the rod according to the TEM image (Fig. 3b). When the reaction time is prolonged to 30 min, the rods change into hollow rods as shown in Fig. 3c. Fig. 3d is the high magnification TEM image of a single hollow rod, which clearly shows the hollow structure in the rod. When the reaction time increases to 2 h, hollow rods with a larger size form, as shown in Fig. 2. It is well-known that the hexagonal ZnO crystal has both polar and nonpolar faces. The typical crystal habit exhibits a basal polar oxygen plane $(000\bar{1})$, top tetrahedron corner-exposed polar zinc plane (0001), and low-index faces (parallel to the *c* axis) consisting of a nonpolar $\{10\bar{1}0\}$ face. Polar faces with surface dipoles are thermodynamically less stable than nonpolar faces, often undergoing rearrangement to

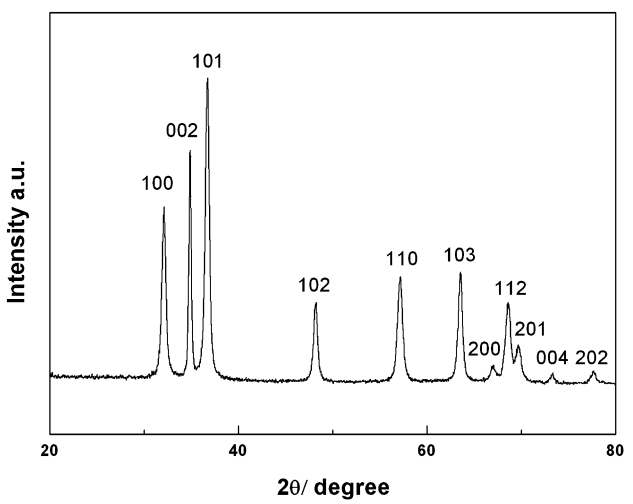

Fig. 1 XRD pattern of a sample precipitated with 10 mg of zinc acetate dihydrate in 0.5 g TEAH ionic liquid with 0.5 g added water.

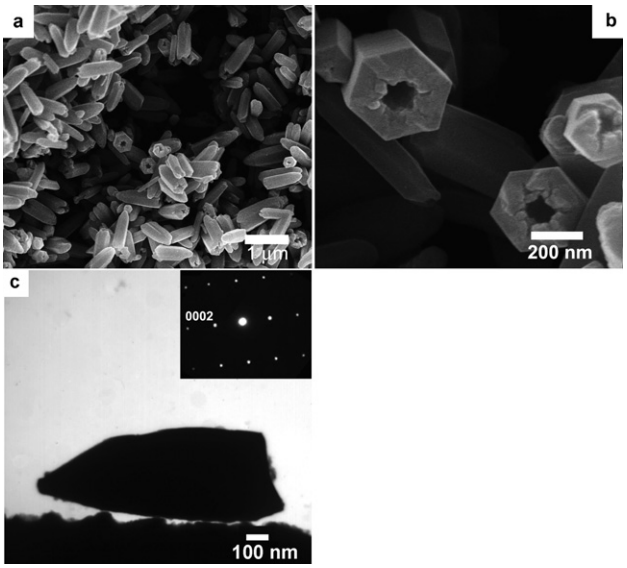

Fig. 2 SEM and TEM images of a sample precipitated with 10 mg of zinc acetate dihydrate in 0.5 g TEAH ionic liquid solution with 0.5 g added water. (a) Low magnification SEM, (b) high magnification SEM, (c) TEM image and a selected area electron diffraction pattern.

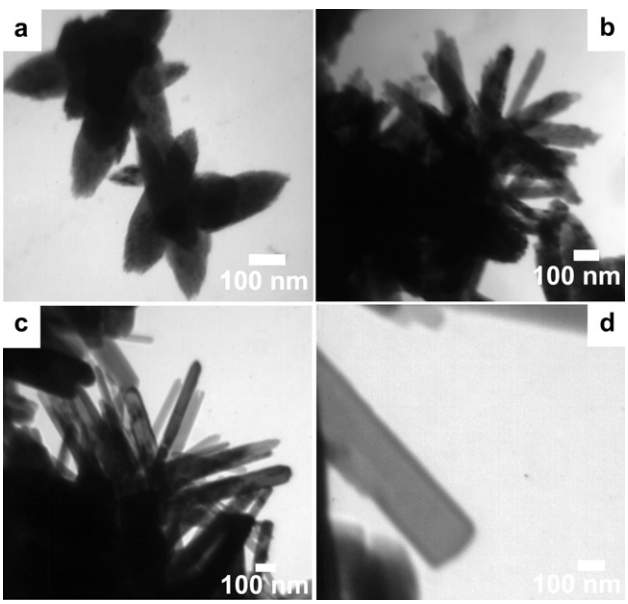

Fig. 3 TEM images of samples precipitated at different reaction times with 10 mg zinc acetate dihydrate in 0.5 g TEAH ionic liquid solution with 0.5 g added water. (a) 5 min, (b) 10 min, (c, d) 30 min.

reduce their surface energy, and usually growing more rapidly.[29] At the early stage of the reaction system, the zinc ions in the solution near the surface of ZnO nuclei adsorb on the polar face of ZnO, resulting in faster growth along the [0001] direction, and thus, ZnO nanorods were obtained. The fast growth causes the Ostwald ripening only to affect slightly the ZnO crystal morphology. With the increase of reaction time, the zinc ions in the solution can be largely consumed. After the growth of ZnO rods reaches a certain equilibrium, the dissolution effect becomes more dominant. Since the polar plane (0001) of ZnO has a higher surface energy, the dissolution rate of the polar plane (0001) is faster than that of the nonpolar plane $\{10\bar{1}0\}$. In addition, the tetrabutylammonium cation will adsorb on the lateral surfaces due to the electrostatic interaction, which will slow down the dissolving velocity of the lateral surfaces. Therefore, the selective dissolution of ZnO causes formation of the hollow structure in the final products. This formation mechanism is different from our previously synthesized ZnO mesocrystals in TBAH ionic liquid, which is based on the assembly of the primary nanoparticle subunits sometimes resulting in a hollow structure.[24]

To understand the influence of the amount of added water in the TEAH ionic liquid solution on the final products, we performed experiments with different amounts of added water in 0.5 g of TEAH solution at a fixed amount of zinc acetate dihydrate (10 mg). Fig. 4 shows SEM images of samples obtained for the products recovered at the conditions with various added water (0, 2.5, 4, 6 g) to the original TEAH solution. In the condition of the original TEAH solution (0 g added water), the particles are quasi-nanospheres (not quite in a spherical shape) with the size ranging from 20 to 50 nm, which is shown in Fig. 4a. Fig. 4b shows the products recovered at the condition with 2.5 g added water which demonstrates that flower-like ZnO particles form with an average size of *ca.* 1 μm. The flower-like particles are constructed of rod particles with the widest rod diameter ranging from *ca.* 300 to 700 nm. Fig. 4c is the higher magnification SEM image for one flower-like particle. It is clearly shown that the tip of the rods has a rough surface resulting in a ladder-like surface. When the amount of added water increases to 4 g, ZnO flower-like particles still form with an average size of *ca.* 800 nm, as shown in Fig. 4d and e. The rod in the flower-like particles is with the widest diameter from *ca.* 150 to 350 nm. Also, the rod has a rough surface which is similar to our previous report about the ZnO particles from the TBAH ionic liquid.[28] Further increasing the added water amount to 6 g, it is found that the product is similar to that recovered at 4 g water. Flower-like particles still form with an average size of 2 μm and the widest diameter of the rod is from 400 to 600 nm, as shown in Fig. 4f.

In order to understand the influence of the zinc acetate dihydrate amount on the final products, we perform experiments at different zinc acetate dihydrate amounts in 0.5 g TEAH ionic liquid solution with 2 g added water. Fig. 5 shows SEM images of samples obtained at 10, 20, 30, and 40 mg zinc acetate dihydrate. At 10 mg zinc acetate dihydrate, the particles are rods with the length ranging from 400 to 800 nm and the diameter ranging

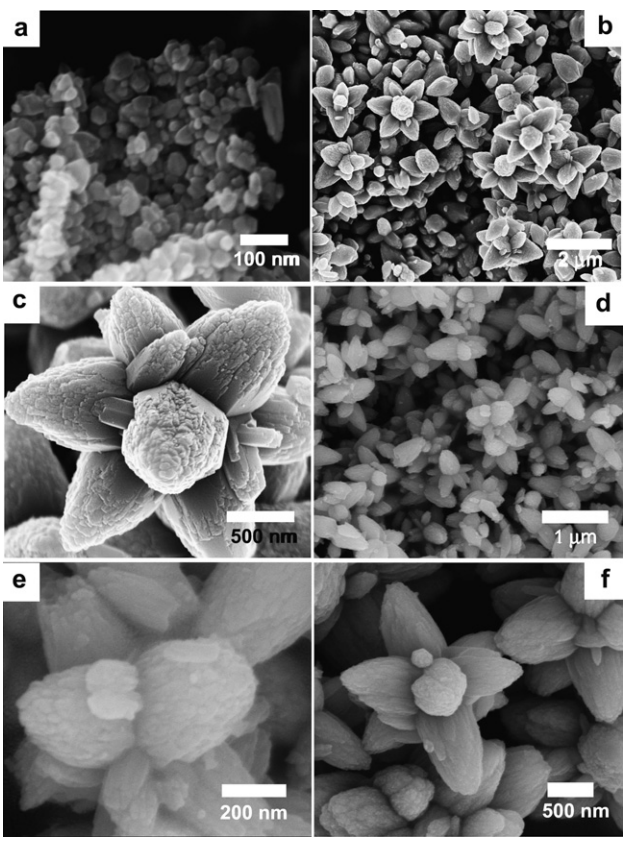

Fig. 4 SEM images of the samples precipitated at various amounts of added water to 0.5 g TEAH ionic liquid solution with a fixed amount of zinc acetate dihydrate (10 mg). (a) 0 g added water, (b, c) 2.5 g added water, (d, e) 4 g added water, (f) 6 g added water.

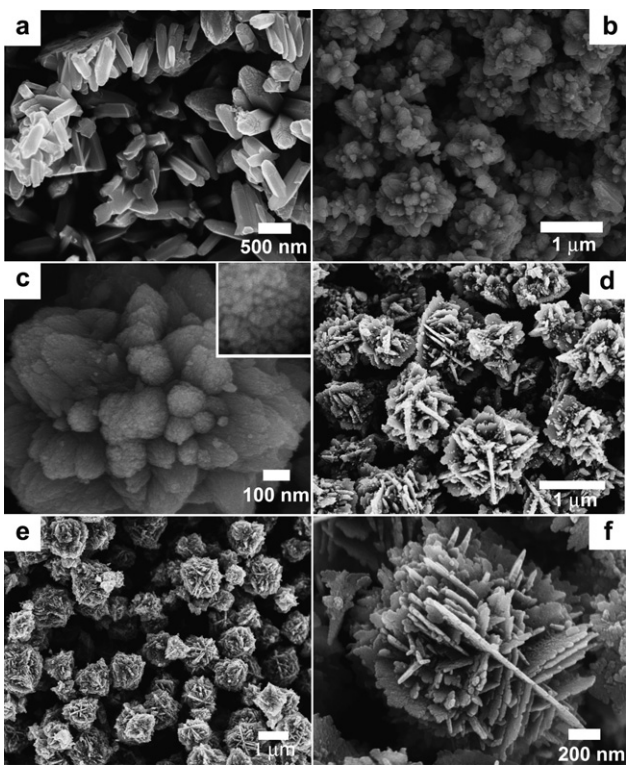

Fig. 5 SEM images of the samples precipitated at different amounts of zinc acetate dihydrate with 2 g of added water in 0.5 g TEAH solution. (a) 10 mg, (b, c) 20 mg, (d) 30 mg, (e, f) 40 mg.

from 150 to 350 nm, which is shown in Fig. 5a. Fig. 5b shows the products recovered at 20 mg zinc acetate dihydrate, which demonstrates that flower-like ZnO particles form with the size ranging from *ca.* 0.5 to 1.2 μm. The flower-like particles are constructed by rod particles with the widest diameter ranging from 100 to 300 nm (Fig. 5c). However the flower-like morphology is different from the result in Fig. 4b because there are much more rods in the flower-like particles in Fig. 5c than in those of the products in Fig.4b. The insert SEM image in Fig. 5c is the higher magnification SEM image for part of the rod surface. It is clearly shown that the rod has a rough surface which is indeed constructed by small nanoparticle subunits with an average size of 10 nm. With further increasing the zinc acetate dihydrate amount to 30 mg, it is found that porous ZnO microspheres form which are constructed of plates (as shown in Fig. 5d). The size of the microspheres is from 0.8 to 1.5 μm and the pore size (the pore size is defined as the distance between two neighbour plate) is from 50 to 260 nm based on the SEM image. The thickness of the plate is *ca.* 50 nm. When the zinc acetate dihydrate amount increases to 40 mg, porous micropheres still form with a size ranging from 0.8 to 1.6 μm (as shown in Fig. 5e). A higher magnification of the SEM image corresponding to one micrsphere in Fig. 5e clearly shows the porous structure and the assemble details in the microsphere (as shown in Fig. 5f). The average thickness of the plate is *ca.* 40 nm and the pore size is from 30 to 200 nm. The capture of the initial particles for these microspheres to demonstrate the formation mechanism has failed, because plate- assembled microspheres already formed when the solution became turbid within 1 min. However, based on this, the formation process might be the following: first the plate ZnO nanoparticles form and in the meanwhile these ZnO plates assemble into spheres, quickly resulting in a porous structure.

The formation mechanism of flower-like particles of which the rods are composed of nanoparticle subunits can be explained as follows. The intrinsic electric fields of the polar ZnO lattice where the crystallographic *c*-axis is polar, could be responsible for the formation of our observed anisotropic structures. The ZnO crystal lattice can be described as alternating planes composed of Zn^{2+} and O^{2-} which are stacked alternatively along the crystallographic *c*-axis. The oppositely charged ions form positively charged (0001)–Zn and negatively charged (0001)–O polar surfaces on the top and on the bottom surface of the primary particles. The assembly of the primary particles is driven by electrostatic interactions from the polar charges to minimize the energy contributed by surface area and polar charges. The presence of large tetrabutylammonium cation of TBAH can reverse the polarity of the negatively charged surfaces of primary particles and thereby prevent further growth and aid the aggregation into flower-like particles. This formation mechanism is similar to our previously synthesized ZnO mesocrystals from TBAH ionic liquid precursor.[24,28]

Also, we perform the experiments in a wide range with the amount of zinc acetate dihydrate from 10 to 40 mg and with added water from 0 to 6 g in 0.5 g TEAH ionic liquid solution. The results are summarized in Table 1. In order to show the heterogeneous structure of the crystalline domain for the synthesized particles, the coherence lengths (crystallite sizes, D_{hkl} where D_{hkl} is the coherence length of the crystalline domain perpendicular to the respective *hkl* plane) are calculated *via* the Scherrer equation according to the peaks of XRD patterns. The results of D_{100}/D_{002} are shown in Table 1. In most cases, the values of D_{100}/D_{002} are completely different from what is observed in electron microscopy. Therefore it suggests that most particles do not consist of only one single crystalline domain, but of several primary subunits.

Table 1 The experiment results for the products recovered in a wide range amounts of zinc acetate dihydrate (10–40 mg) and added water (0–6 g) in 0.5 g TEAH ionic liquid solution. D_{hkl} is the coherence length of the crystalline domain perpendicular to the respective *hkl* plane

Zinc acetate dihydrate/mg	Added water amount/g	Morphology	D_{100}/D_{002}
10	0	Quasi-nanospheres	0.76
10	0.5	Hollow rods	0.38
10	2	Rods	0.35
10	2.5	Flower-like particles constructed by rods	0.66
10	4	Flower-like particles constructed by rods	0.51
10	6	Flower-like particles constructed by rods	0.73
20	0	Rods+quasi-nanospheres	0.51
20	0.5	Rods+quasi-nanospheres	0.55
20	2	Flower-like particles constructed by rods	0.89
20	2.5	Flower-like particles constructed by rods	0.90
20	4	Plate aggregates	0.73
20	6	Flower-like particles constructed by rods	0.85
30	0	Rods+quasi-nanospheres	0.69
30	0.5	Plates	0.45
30	2	Porous microspheres conctructed by plates	0.89
30	2.5	Porous microspheres conctructed by plates	0.90
30	4	Plate aggregates	0.88
30	6	Flower-like particles constructed by rods	0.92
40	0	Rods+quasi-nanospheres	0.55
40	0.5	Plates	0.65
40	2	Porous microspheres conctructed by plates	0.76
40	2.5	Porous microspheres conctructed by plates	0.81
40	4	Flower-like particles constructed by rods	0.90
40	6	Porous microspheres conctructed by plates	0.91

There have been reports on the growth of ZnO from ionic liquid precursors. Zhu *et al.* have reported that zinc-containing ILs can be utilized as zinc oxide precursors for the growth of ZnO *via* an ionothermal process.[20] There, a zinc/amine complex was reacted with tetramethylammonium hydroxide, in a water-free environment. Under these conditions, ZnO multipods were obtained. We have recently shown that the highly hydrated IL tetrabutylammonium hydroxide (TBAH) is an efficient ILP for the fabrication of unusual ZnO mesocrystals *via* the reaction of zinc acetate with TBAH by the reflux method or in the open air.[24,25,28] Tubular rods with a rough surface and "lotus leaf-like"

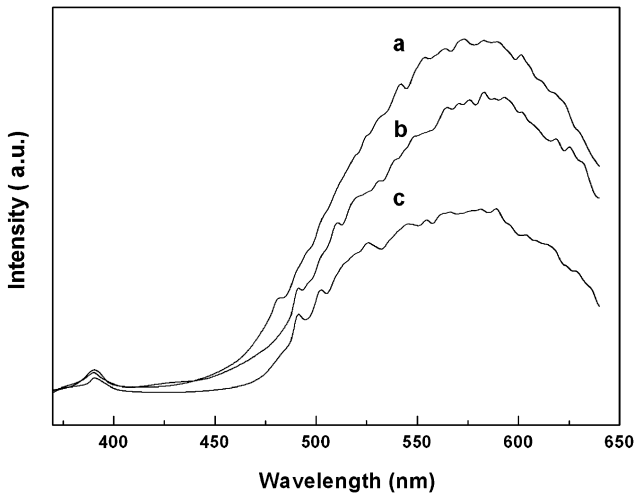

Fig. 6 Room temperature photoluminescence spectra for typical samples. (a) Porous microspheres conctructed of plates, (b) flower-like particles constructed of rods, (c) hollow rods.

particles form in the TBAH ionic liquid. In the present study, the hollow rods from TEAH are with a smooth surface which is different from the products obtained in TBAH. Also, porous microspheres constructed of plates can form in TEAH. The mechanism for the hollow rods formed in TBAH and TEAH is different. In TBAH the formation of hollow rods is based on the assembly of the primary nanoparticle subunits while in TEAH the formation of hollow rods results from the selective dissolution of the initial rods.

Fig. 6 shows room-temperature photoluminescence (PL) spectra for typical synthesized ZnO products. Photoluminescence at room temperature shows a broad green fluorescence peak centered at around 575 nm for all samples. A smaller peak at 390 nm can be assigned to the bandgap luminescence of ZnO from exciton transitions. The band at 575 nm can be assigned to recombination processes from deep levels in the bandgap of ZnO. These deep levels are well-known to be especially pronounced in ZnO obtained *via* low-temperature fabrication processes.[24] In the current case the defects are likely related to oxygen defects in the ZnO lattice. This PL spectroscopy thus shows that the optical properties of the synthesized ZnO products are largely governed by the number and nature of the defects in the ZnO lattice, which is similar to our previously synthesized ZnO particles in the TBAH ionic liquid.[24,28]

Conclusion

In conclusion, this paper is another contribution to the synthesis of inorganic nanostructured materials from an ionic liquid precursor. Like the TBAH ionic liquid, the present work shows that tetraethylammonium hydroxide (TEAH) is also an efficient ILPs for the controlled fabrication of zinc oxide particles with various shapes and sizes. ZnO particles with interesting multi-shapes can be obtained by the present route. The synthesized nanostructured ZnO includes: hollow ZnO rods, flower-like ZnO particles constructed of rods with nanoparticle subunits and porous ZnO microspheres assembled from ZnO nanoplates. PL measurements reveal that the as-obtained ZnO nanostructures exhibit intense green emission which demonstrates there is a large amount of defects in the ZnO lattice. These ZnO particles with controlled morphology and size may be useful for many applications including catalysis.

Acknowledgements

This work is supported by the National Natural Science Foundation of China (NSFC, No.20803043, No.20803044, No. 50772061).

References

1 R. Sheldon, *Chem. Commun.*, 2001, 2339.
2 J. G. Huddleston, H. D. Willauer, R. P. Swatloski, A. E. Visser and R. D. Rogers, *Chem. Commun.*, 1998, 1765.
3 E. V. Dickinson, M. E. Williams, S. M. Hendrickson, H. Masui and R. W. Murray, *J. Am. Chem. Soc.*, 1999, **121**, 613.
4 M. Antonietti, D. Kuang, B. Smarsly and Y. Zhou, *Angew. Chem., Int. Ed.*, 2004, **43**, 4988.
5 A. Taubert, *Acta Chim. Slov.*, 2005, **52**, 183.
6 A. Taubert and Z. Li, *Dalton Trans.*, 2007, (7), 723.
7 Z. Li, Z. Jia, Y. Luan and T. Mu, *Curr. Opin. Solid State Mater. Sci.*, 2008, **12**, 1.
8 Z. Li, Z. Liu, J. Zhang, B. Han, J. Du, Y. Gao and T. Jiang, *J. Phys. Chem. B*, 2005, **109**, 14445.
9 Y. Zhu, W. Wang, R. Qi and X. Hu, *Angew. Chem., Int. Ed.*, 2004, **43**, 1410.
10 D. Batra, S. Seifert, L. M. Varela, A. C. Y. Liu and M. A. Firestone, *Adv. Funct. Mater.*, 2007, **17**, 1279.
11 Y. Wang and H. Yang, *J. Am. Chem. Soc.*, 2005, **127**, 5316.
12 K. Ding, Z. Miao, Z. Liu, Z. Zhang, B. Han, G. An, S. Miao and Y. Xie, *J. Am. Chem. Soc.*, 2007, **129**, 6362.
13 Z. Li, A. Friedrich and A. Taubert, *J. Mater. Chem.*, 2008, **18**, 1008.
14 E. Redel, R. Thomann and C. Janiak, *Chem. Commun.*, 2008, 1789.
15 A. Taubert, *Angew. Chem., Int. Ed.*, 2004, **43**, 5380.
16 A. Taubert, *Acta Chim. Slov.*, 2005, **52**, 168.
17 A. Taubert, P. Steiner and A. Mantion, *J. Phys. Chem. B*, 2005, **109**, 15542.
18 A. Taubert, C. Palivan, O. Casse, F. Gozzo and B. Schmitt, *J. Phys. Chem. C*, 2007, **111**, 4077.
19 A. Taubert, I. Arbell, A. Mecke and P. Graf, *Gold Bull.*, 2006, **39**, 205.
20 H. Zhu, J.-F. Huang, Z. Pan and S. Dai, *Chem. Mater.*, 2006, **18**, 4473.
21 K. S. Kim, S. Choi, J. H. Cha, S. H. Yeon and H. Lee, *J. Mater. Chem.*, 2006, **16**, 1315.
22 J. Liang, S. Bai, Y. Zhang, M. Li, W. Yu and Y. Qian, *J. Phys. Chem. C*, 2007, **111**, 1113.
23 Z. Dai, K. Liu, Y. Tang, X. Yang, J. Bao and J. Shen, *J. Mater. Chem.*, 2008, **18**, 1919.
24 Z. Li, A. Geßner, J. Richters, J. Kalden, T. Voss, C. Kubel and A. Taubert, *Adv. Mater.*, 2008, **20**, 1279.
25 Z. Li, A. Shkilnyy and A. Taubert, *Cryst. Growth Des.*, 2008, **8**, 4526.
26 Z. Li, P. Rabu, P. Strauch, A. Mantion and A. Taubert, *Chem.–Eur. J.*, 2008, **14**, 8409.
27 Z. Li, Y. Z. Khimyak and A. Taubert, *Materials*, 2008, **1**, 3.
28 Z. Li, Y. Luan, T. Mu and G. Chen, *Chem. Commun.*, 2009, 1258.
29 Q. Yu, W. Fu, C. Yu, H. Yang, R. Wei, M. Li, S. Liu, Y. Sui, Z. Liu, M. Yuan, G. Zou, G. Wang, C. Shao and Y. Liu, *J. Phys. Chem. C*, 2007, **111**, 17521.